J. Meas. Sci. Instrum., 2024, 15(3): 379-386. http://jmsi.publish.founderss.cn/
DOI: 10.62756/jmsi.1674-8042.2024039 jmsi@nuc.edu.cn

Design and verification of an improved experimental platform for stray current in urban rail transit

LI Yaning[1*], KANG Hong[1], WANG Ye[2], LI Wenfei[1], JIAO Meng[1], ZHANG Wencai[1]

1. School of Automation and Electrical Engineering, Lanzhou Jiaotong University, Lanzhou 730070, China;
2. School of Environmental and Municipal Engineering, Lanzhou Jiaotong University, Lanzhou 730070, China

***Corresponding author:** LI Yaning (liyaning@mail.lzjtu.cn)

Received: October 3, 2023 **Revised:** December 18, 2023 **Accepted:** January 4, 2024

Abstract: With the rapid development of urban rail transit, there have been an urgent problem of excessive stray current. Because the stray current distribution is random and difficult to verify in the field, we designed an improved stray current experimental platform by replacing the simulated aqueous solution with a real soil environment and by calculating the transition resistance by measuring the soil resistivity, which makes up for the defects in the previous references. Firstly, the mathematical models of rail-drainage net and rail-drainage net-ground were established, and the analytical expressions of current and voltage of rail, drainage net and other structures were derived. In addition, the simulation model was built, and the mathematical analysis results were compared with the simulation results. Secondly, the accuracy of the improved stray current experimental platform was verified by comparing the measured and simulation results. Finally, based on the experimental results, the influence factors of stray current were analyzed. The relevant conclusions provide experimental data and theoretical reference for the study of stray current in urban rail transit.

Key words: urban rail transit; stray current; experimental platform; transition resistance; soil resistivity

0 Introduction

Urban rail transit has the characteristics of convenience, high passenger volume and high safety, which is one of the main development directions of modern rail transit[1-3]. The traction power supply system of urban rail transit generally adopts the power supply mode of catenary or the third rail to supply power to the train and the current is back to the substation along the rail[4,5]. As the complete insulation between the rail and the earth cannot be achieved, part of the return current will leak to the periphery to form stray current[6,7], as shown in Fig. 1. Stray current has strong instantaneity and randomness, and its size is usually several milliamps to several amps, which is difficult to measure in the lines that have been put into operation. In some lines with poor insulation, the instantaneous peak value of stray current can even reach more than 2 000 A, resulting in frequent action and even locking of rail over-voltage protection device (OVPD) [8]. Stray current will cause corrosion and perforation of buried metal pipelines, cause DC bias of grounding transformers and increase reactor harmonics, which will bring serious hidden dangers to the normal operation of urban rail transit power supply system and urban power grid[9,10].

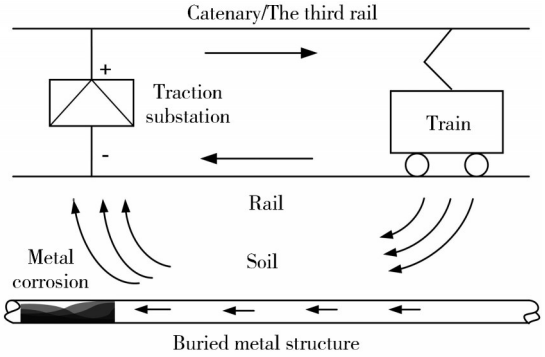

Fig. 1 Stray current generation process

In recent years, scholars have done many researches on the problem of stray current. Ogunsola et al.[11-13] layered the return circuit of urban rail transit power supply system, and constructed a mathematical differential equation according to the relationship between voltage and current at each point. The influence and distribution of stray current caused by variables such as rail longitudinal resistance were simulated and analyzed. Du et al.[14,15] combined the power flow calculation of urban rail transit power supply system with the stray current distribution model to establish a simulation model and analyze the dynamic distribution law

of stray current and rail potential under the condition of multi train operation. Charlamabous et al.[16] used computer-aided design of grounding systems (CDEGS) to build the stray current distribution model under tunnel conditions, and evaluated the stray current under train regenerative braking. Li et al.[17,18] established a stray current monitoring system, but the real soil environment was not used in the experiment, and there was a lack of equivalent calculation of rail-ground transition resistance under experimental conditions.

In this study, the mathematical models of rail-ground and rail-drainage net-ground were derived, and then the simulation model was established to compare the mathematical analysis results with the simulation results to verify the rationality of the simulation model. Furthermore, an improved stray current experimental test platform was built to replace the simulated aqueous solution with the real soil, and the rail earth transition resistance and rail drainage network transition resistance were calculated by measuring the soil resistivity. In the experiment, eight resistances with equal resistance values were connected in series to simulate the rail, and the connection points at both ends of the resistance were connected with the upper end of the data acquisition module, and the lower end was connected with the probe inserted into the soil. After the power was turned on, the current flowed through the resistance in turn to produce a voltage drop and form a leakage current. The leakage current was measured by the data acquisition module before flowing into the soil, and the stray current was calculated according to the measured leakage current. Finally, based on the experimental results, the influence factors of stray current were analyzed.

1 Mathematical model of stray current

1.1 Model construction

The rail and the drainage network structure are equivalently cut by infinitesimal elements, and the traction substation and the train are equivalent to the current source and voltage source under ideal conditions respectively, and the other parts are replaced by equivalent resistance, then the rail-ground and rail-drainage net-ground stray current distribution models can be constructed, as shown in Fig.2.

In Fig.2, L is the section length, I_s is the rail current, I_r is the drainage net current, u_g is the rail drainage net voltage, u_p is the drainage network earth voltage, R_s is the rail longitudinal resistance, R_r is the drainage net longitudinal resistance, R_d is the rail-ground transition resistance, R_g is the rail-drainage-net transition resistance, and R_p is the drainage net-ground transition resistance. It is assumed that R_d, R_g and R_p are uniformly distributed, and the catenary resistance r is ignored.

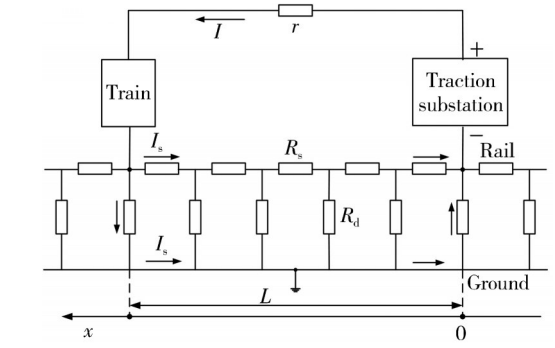

(a) Rail-ground structure model

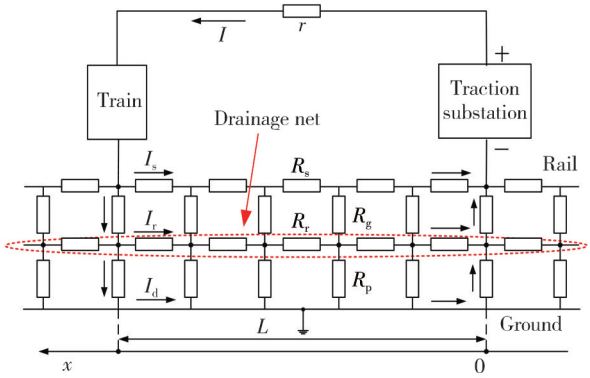

(b) Rail-drainage net-ground structure model

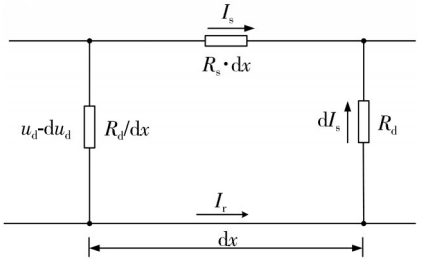

(c) Rail-ground infinitesimal structure

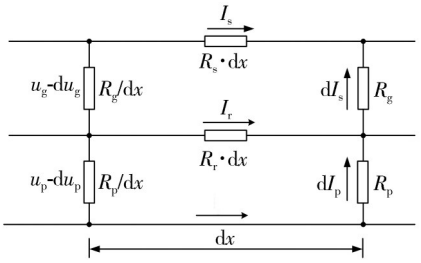

(d) Rail-drainage net-ground infinitesimal structure

Fig. 2 Stray current distribution model

1.2 Model of rail-ground

The double-layer differential structure is shown in Fig.2(c). According to Kirchhoff's law, the following differential equations can be obtained as

$$\begin{cases} \mathrm{d}u_d = I_s R_s \,\mathrm{d}x, \\ \mathrm{d}I_d = \dfrac{u_d}{R_d}\mathrm{d}x. \end{cases} \tag{1}$$

Eq.(1) can be rewritten as

$$I_s = A_1 e^{\lambda x} + A_2 e^{-\lambda x}, \tag{2}$$

where $\lambda = \sqrt{R_s/R_d}$, and A_1 and A_2 are undetermined coefficients.

On an ideal boundary condition that

$$\begin{cases} I_s(0) = I, \\ I_s(L) = I. \end{cases} \tag{3}$$

When Eq. (3) is substituted into Eq. (2), we can get

$$\begin{cases} A_1 = \dfrac{I}{1 + e^{\lambda L}}, \\ A_2 = \dfrac{I e^{\lambda L}}{1 + e^{\lambda L}}. \end{cases} \tag{4}$$

Combined with Eqs. (1) — (4), we can calculate the stray current by

$$I_1 = I\left(1 - \frac{e^{\lambda x} + e^{\lambda L} e^{-\lambda x}}{1 + e^{\lambda L}}\right). \tag{5}$$

1.3 Model of rail-drainage net-ground

The three-layer differential structure is shown in Fig. 2(d). According to Kirchhoff's law, the differential equations can be obtained as

$$\begin{cases} \mathrm{d}u_g = I_s R_s \,\mathrm{d}x - I_r R_r \,\mathrm{d}x, \\ \mathrm{d}u_p = I_r R_r \,\mathrm{d}x, \\ \mathrm{d}I_s = \dfrac{u_g}{R_g}\,\mathrm{d}x, \\ \mathrm{d}I_r = \dfrac{u_p}{R_p}\,\mathrm{d}x - \dfrac{u_g}{R_g}\,\mathrm{d}x. \end{cases} \tag{6}$$

Futhermore, we can get

$$\begin{cases} I_s = C_1 e^{\lambda_1 x} + C_2 e^{-\lambda_1 x} + C_3 e^{\lambda_2 x} + C_4 e^{-\lambda_2 x}, \\ I_r = k_1 C_1 e^{\lambda_1 x} + k_1 C_2 e^{-\lambda_1 x} + k_2 C_3 e^{\lambda_2 x} + k_2 C_4 e^{-\lambda_2 x}, \end{cases} \tag{7}$$

where

$$\begin{cases} \lambda_1 = \sqrt{\dfrac{1}{2}\left[\left(\dfrac{R_s + R_r}{R_g} + \dfrac{R_r}{R_p}\right) + \sqrt{\left(\dfrac{R_s + R_r}{R_g} + \dfrac{R_r}{R_p}\right)^2 - 4\dfrac{R_s R_r}{R_g R_p}}\right]}, \\ \lambda_2 = \sqrt{\dfrac{1}{2}\left[\left(\dfrac{R_s + R_r}{R_g} + \dfrac{R_r}{R_p}\right) - \sqrt{\left(\dfrac{R_s + R_r}{R_g} + \dfrac{R_r}{R_p}\right)^2 - 4\dfrac{R_s R_r}{R_g R_p}}\right]}, \\ k_1 = \dfrac{R_s - \lambda_1^2 R_g}{R_p}, \\ k_2 = \dfrac{R_s - \lambda_2^2 R_g}{R_p}. \end{cases} \tag{8}$$

and C_1, C_2, C_3, C_4, k_1 and k_2 are undetermined coefficients.

According to an ideal boundary condition that

$$\begin{cases} I_s(0) = I, \\ I_r(0) = 0, \\ I_s(L) = I, \\ I_r(L) = 0. \end{cases} \tag{9}$$

When Eq. (9) is substituted into Eq. (7), we can get

$$\begin{cases} C_1 = \dfrac{k_1 I}{1 + e^{\lambda_1 L}}, \\ C_2 = \dfrac{k_1 I e^{\lambda_1 L}}{1 + e^{\lambda_1 L}}, \\ C_3 = \dfrac{k_2 I}{1 + e^{\lambda_2 L}}, \\ C_4 = \dfrac{k_2 I e^{\lambda_2 L}}{1 + e^{\lambda_2 L}}, \\ k_1 = \dfrac{R_s - \lambda_2^2 R_g}{(\lambda_1^2 - \lambda_2^2) R_g}, \\ k_2 = \dfrac{R_s - \lambda_1^2 R_g}{(\lambda_2^2 - \lambda_1^2) R_g}. \end{cases} \tag{10}$$

Combined with Eqs. (6) — (10), the stray current is calculated by

$$I_s = I\left[1 - \frac{(1 + k_1)(R_s - \lambda_2^2 R_g)(e^{\lambda_1 x} + e^{\lambda_1 L} e^{-\lambda_1 x})}{(\lambda_1^2 - \lambda_2^2) R_g (1 + e^{\lambda_1 L})} - \frac{(1 + k_2)(R_s - \lambda_1^2 R_g)(e^{\lambda_2 x} + e^{\lambda_2 L} e^{-\lambda_2 x})}{(\lambda_2^2 - \lambda_1^2) R_g (1 + e^{\lambda_2 L})}\right]. \tag{11}$$

2 Construction and verification of stray current simulation model

Based on the mathematical analytical formulas of the two models obtained above, the simulation model was constructed in Matlab. To verify the accuracy and reliability of the simulation model, all the parameters in the analytical calculation and the simulation model were set to be equal, and then the analytical calculation results were compared with the simulation results.

The comparison between the analytical results and the simulation results is shown in Fig. 3. In the analytical calculation, simulation and experiment, the value of L is the length of the experimental vessel, the resistance value of R_s is the same as the resistance value used in the experiment, the value of R_r is the same as the longitudinal resistance value of the drainage net used in

the experiment, and the settings of R_d and R_g were calculated by the soil resistivity of the experimental soil. The settings of specific parameters are shown in Table 1.

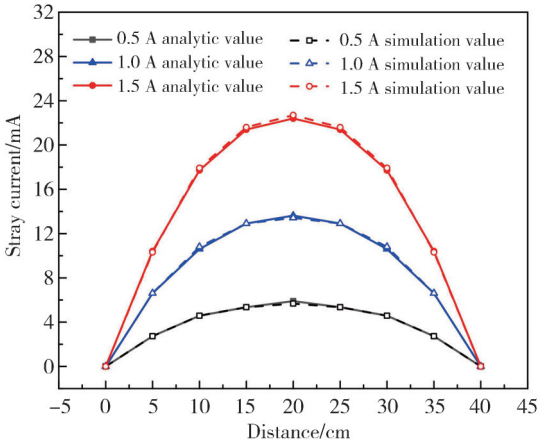

(a) Rail-ground model

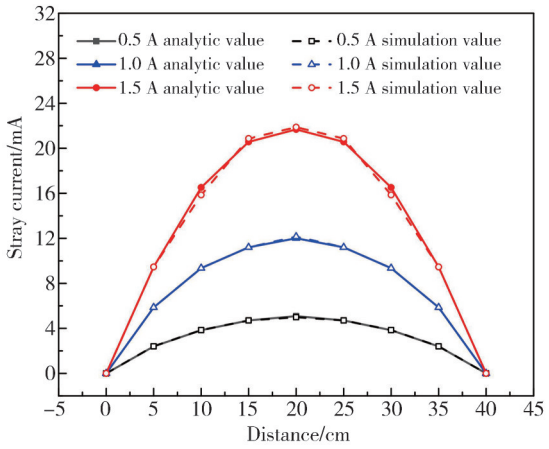

(b) Rail-drainage net-ground model

Fig. 3 Comparison of analytical and simulation results

Table 1 Parameter settings

Parameter	Value
L/cm	40
R_s/(Ω•cm^{-1})	1
R_r/(Ω•cm^{-1})	0.01
R_d/(Ω•cm^{-1})	35
R_g/(Ω•cm^{-1})	35

In the rail-ground model and rail-drainage net-ground model, when the traction current is 1.5 A, there is a certain error between the simulation value and the analytic value, and the maximum relative deviation is not more than 3.9%. When the traction currents is 0.5 A and 1.0 A, the analytic values are basically consistent with the simulation values, which proves the accuracy and reliability of the simulation model.

3 Design and verification of improved experimental platform

3.1 Experimental principle

To analyze the distribution of stray current in soil, an improved stray current experimental platform was established in combination with Refs. [17-20]. In the experiment, the simulated aqueous solution was replaced by the real soil environment, and the drainage net structure was added in the rail drainage-net-ground model experiment. The soil resistivity was measured and converted into equivalent R_d and R_g through calculation, which makes up for the deficiencies in the literature and makes the experimental platform closer to the engineering practice. The experimental schematic diagram is shown in Fig. 4, and the connection diagram of the experimental platform is shown in Fig. 5.

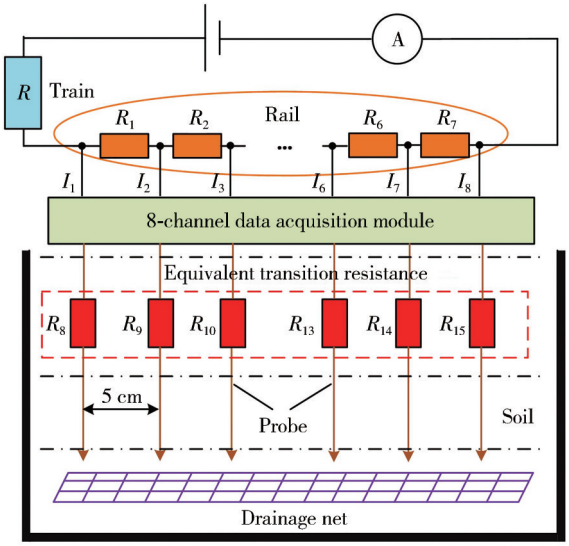

Fig. 4 Experimental schematic diagram

(a) Stray current experimental platform

(b) Drainage net structure

Fig. 5 Connection diagram of experimental platform

In the simulation experiment, Faith FT10010 linear DC power supply simulated the traction substation,

resistance R simulated the train, $R_1 - R_7$ simulated the rail resistance, and $R_8 - R_{15}$ simulated the equivalent R_d and R_g. The model of data acquisition module is DAQM-4202 of Zhouzheng Technology. Its current and voltage measurement ranges are ±20 mA and ±500 mV, respectively, and the accuracy grade is ± 1‰, which meets the needs of the experiment. When carrying out the rail-drainage net-ground model experiment, a reinforcing mesh with a length of 42.5 cm and a width of 30 cm was embedded, as shown in Fig.5 (b).

The metal probe with radius r_1 of 0.000 1 m was inserted into the compacted soil, and the upper end was connectedwith the data acquisition module. The distance r_2 between adjacent probes was 5 cm, and the total length of the simulation interval was 0.4 m. The measured current value was the leakage current value, and the stray current calculation was the sum of leakage currents at each point.

The resistivity of the soil used in the experiment was measured by 4 pole method[21]. The measurement principle is shown in Fig.6. The size parameters of each polar plate and insulated container in the soil resistivity measurement experiment are shown in Table 2.

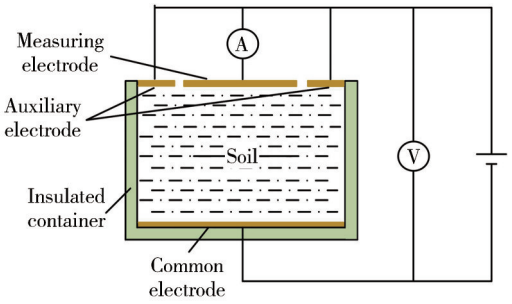

Fig. 6 Schematic diagram of soil resistivity measurement

Table 2 Parameters of dimensions of each polar plate and insulating container

Type	Size/cm
Common electrode	15×15
Measuring electrode	8×8
Auxiliary electrode	2×8
Insulated container	15×15×15

From $R = \rho L/S$ and $i = U/R$, the resistivity of soil samples can be deduced as

$$\rho = \frac{US}{il}, \tag{12}$$

where U is the reading of voltmeter, i is the reading of ammeter, S is the area of the measuring electrode, and l is the distance between the upper and lower plates.

The equivalent calculation method of R_d and R_g is expressed as

$$R = \frac{\rho}{2\pi} \ln \frac{r_2}{r_1}. \tag{13}$$

3.2 Comparison and verification of experiment and simulation results

According to the 4 pole method, the soil resistivity was measured and solved for three times, and the average value was 45 Ω·m^{-1}. Substituting the value into Eq. (13), R_d and R_g were calculated as 35 Ω·m^{-1}. Finally, the measured R_d and R_g values were brought into the simulation. The drainage net structure used in the experiment was welded by fine steel bars. For the convenience of calculation, the R_r was taken as 0.01 Ω·cm^{-1}[22,23].

The comparison between simulation and measured values is shown in Fig.7.

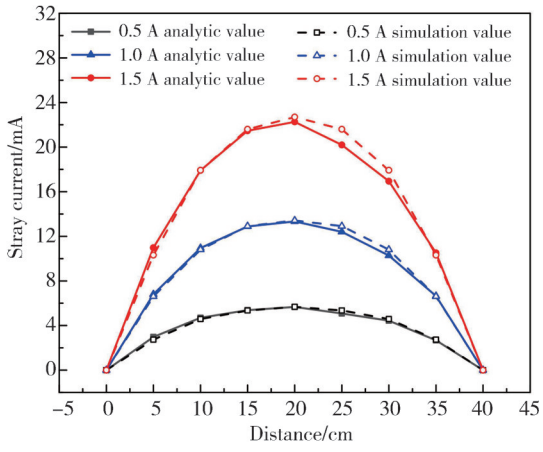

(a) Rail-ground model

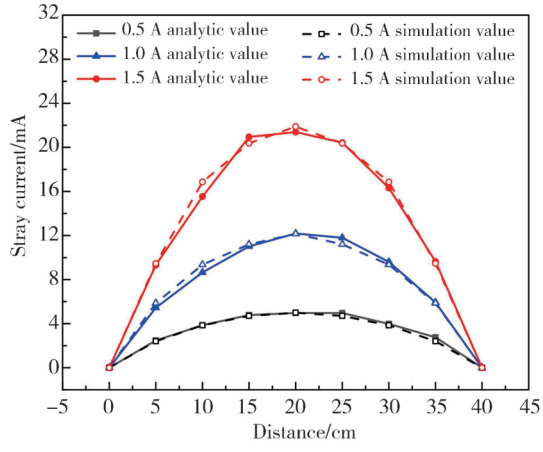

(b) Rail-drainage net-ground model

Fig. 7 Comparison of measured and simulated values

The measured value of stray current of rail-ground model and rail-drainage net-ground model is basically consistent with the simulation value, which proves the accuracy and reliability of the experimental platform. In the rail-ground model, the maximum deviation between the measured value and the simulated value is 0.980 mA, the maximum relative deviation is 5.79%. The minimum deviation is 0.029 mA, and the minimum relative deviation is 0.23%. In the rail-drainage net-

ground model, the maximum deviation between the measured value and the simulated value is 0.705 mA, and the maximum relative deviation is 8.15%. The minimum deviation is 0.027 mA, and the minimum relative deviation is 0.22%. When the traction current is 0.5 A, the consistency between simulation and experimental results is the highest, followed by 1.0 A, and the lowest at 1.5 A. The reason for the experimental deviation may be that the resistance heats up due to the increase of temperature, resulting in the change of resistance value.

4 Influence of various parameters on stray current

Based on the experimental data from the improved stray current experimental platform, the influencing factors of stray current are analyzed. The leakage current and stray current distribution with and without drainage net are shown in Figs.8 and 9, respectively.

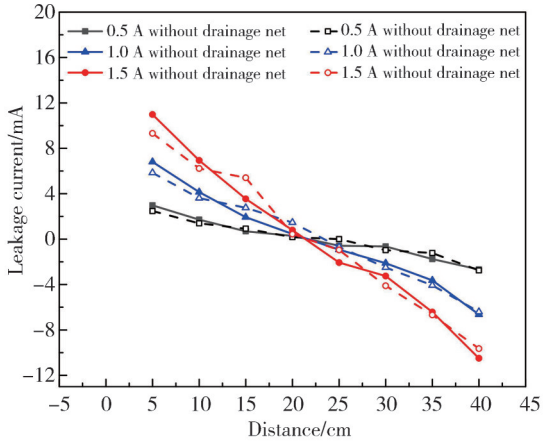

Fig. 8 Comparison of leakage currents with and without drainage net

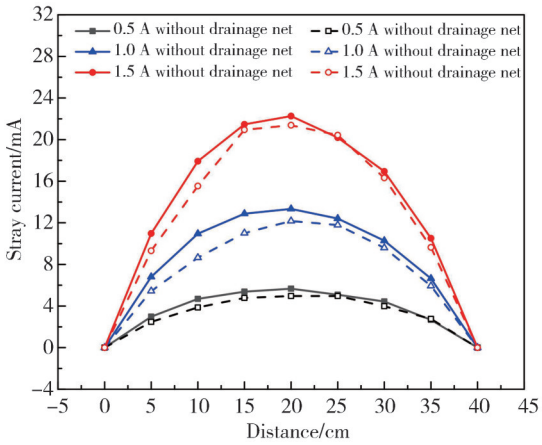

Fig. 9 Comparison of stray currents with and without drainage net

The values of leakage current and stray current at each point are shown in Table 3 and Table 4, respectively.

Table 3 Leakage current values of each point with or without drainage net

Distance/cm	Leakage current/mA					
	Traction current 0.5 A		Traction current 1.0 A		Traction current 1.5 A	
	WODN	WDN	WODN	WDN	WODN	WDN
0	0	0	0	0	0	0
5	2.978	2.475	6.805	5.844	10.979	9.315
10	1.715	1.386	4.146	3.608	6.940	6.228
15	0.688	0.925	1.928	2.764	3.547	5.404
20	0.287	0.178	0.454	1.465	0.796	0.439
25	−0.584	0	−0.927	−0.689	−2.068	−0.956
30	−0.649	−0.977	−2.126	−2.494	−3.254	−4.111
35	−1.760	−1.221	−3.633	−3.254	−6.422	−6.681
40	−2.676	−2.755	−6.642	−6.405	−6.681	−9.644

WDN is the case with drainage net, WODN is the case without drainage net.

Table 4 Stray current values of each point with or without drainage net

Distance/cm	Stray current/mA					
	Traction current 0.5 A		Traction current 1.0 A		Traction current 1.5 A	
	WODN	WDN	WODN	WDN	WODN	WDN
0	0	0	0	0	0	0
5	2.978	2.475	6.805	5.844	10.979	9.315
10	4.693	3.861	10.951	8.652	17.919	15.543
15	5.381	4.786	12.879	11.016	21.466	20.947
20	5.668	4.964	13.333	12.181	22.262	21.386
25	5.084	4.964	12.406	11.792	20.194	20.430
30	4.435	3.987	10.280	9.598	16.940	16.319
35	2.675	2.766	6.647	5.927	10.518	9.638
40	0	0	0	0	0	0

WDN is the case with drainage net, WODN is the case without drainage net.

4.1 Traction current

In the rail-ground model, when the traction current is 0.5 A, 1.0 A and 1.5 A, respectively, the maximum leakage current of the rail ground model is 2.978 mA, 6.805 mA and 10.979 mA, respectively, and the minimum leakage current is − 2.676 mA, − 6.642 mA, and −10.494 mA, respectively. The maximum stray current is 5.668 mA, 13.333 mA and 22.262 mA, respectively, and the minimum value is 0. In the rail-drainage net-ground model, the maximum leakage current is 2.475 mA, 5.844 mA and 9.315 mA, respectively, the minimum leakage current is − 2.676 mA, − 6.642 mA, and −10.494 mA, respectively. The maximum stray current is 4.964 mA, 12.181 mA and 21.386 mA respectively, and the minimum value is 0.

When the distance between the train and the traction substation is the same, with the increase of traction current, the leakage current and stray current also increase, and the increase is obvious. It shows that traction current is one of the important factors affecting leakage current and stray current.

4.2 Distance between train and traction substation

With the same traction current, the leakage current gradually decreases with the increase of the distance between the train and the traction substation, while the stray current increases first and then decreases.

4.3 Drainage net

When the traction current is 0.5 A, 1.0 A and 1.5 A, respectively, the maximum difference of leakage current with and without drainage net is 0.584 mA, 0.961 mA and 1.857 mA, respectively, and the maximum difference of stray current is 0.832 mA, 2.299 mA and 2.376 mA, respectively. After adding the drainage net, the stray current is reduced by 17.73%, 20.99% and 13.26%, respectively.

When the traction currents are the same, the leakage current change little after adding the drainage network structure, while the stray current shows a decreasing trend. It shows that the drainage net has a certain degree of inhibition on stray current. When the traction current is 1.0 A, the drainage net has the most obvious inhibitory effect on stray current.

5 Conclusions

In this study, we designed and verified an improved experimental platform for stray current in urban rail transit by combining mathematical analysis, simulation analysis and experimental verification. The main conclusions are as follows.

1) The meathod of replacing the water solution of the simulated soil with the real soil and calculating the rail earth transition resistance and rail drainage network transition resistance by measuring the soil resistivity, which makes up for the neglect of the solution method of transition resistance in the experimental platform in the previous literature, and makes the experimental conclusion more rigorous and accurate.

2) The maximum deviation between the measured results and the simulation results of the rail-ground model and the rail-drainage net-ground model are 5.79% and 8.15%, respectively, with small errors. It verifies the accuracy and reliability of the improved stray current experimental platform.

3) The traction current, the distance between the train and the traction substation, and the structure of the drainage net all have a certain impact on the stray current.

Acknowledgement

This work was supported by National Natural Science Foundation of China (Nos.51476073, 51266004); Natural Science Foundation of Gansu Province (No.138RJZA199).

Declaration of conflicting interests

The authors have no conflict of interests related to this publication.

References

[1] CHEN W L, LI Y N, WANG Y. Influence of soil resistivity on stray current in urban rail power supply system. Journal of Measurement Science and Instrumentation, 2022, 13(3): 261-266.

[2] WANG F, LIU B F, WANG D L. Status assessment for the urban rail transit preloaded substations based on Matter-Element Extensible Theory. Journal of Railway Science and Engineering, 2020, 17(2): 477-484.

[3] SAHIL B, YANG X F, WANG M, et al. Review and evaluation of stray current mitigation for urban rail transit. Transactions of China Electrotechnical Society, 2021, 36(23): 4851-4863.

[4] GU J D, YANG X F, ZHENG Q L, et al. Rail potential and stray current on negative resistance converter traction power system under different grounding schemes and train conditions. Transactions of China Electrotechnical Society, 2021, 36(23): 4851-4863.

[5] LIN S, WANG A M, LIU M J, et al. A multiple section model of stray current of DC metro systems. IEEE

Transactions on Power Delivery, 2021, 36(3): 1582-1593.
[6] LI Y N, LI M, GAO X H, et al. Simulation and experimental verification of stray current in urban rail transit based on CDEGS modeling. Journal of the China Railway Society, 2021, 43(12): 49-54.
[7] DUAN R. Analysis and solution research on abnormal action of rail potential limiting device. Electric Railway, 2020, 31(6): 73-76.
[8] WANG C T, LI W, WANG Y Q, et al. Chloride-induced stray current corrosion of Q235A steel and prediction model. Construction and Building Materials, 2019, 219: 164-175.
[9] YU K, NI Y R, ZENG X J, et al. Modeling and analysis of transformer DC bias current caused by metro stray current. IEEJ Transactions on Electrical and Electronic Engineering, 2020, 15(10): 1507-1519.
[10] OGUNSOLA A, SANDROLINI L, MARISCOTTI A. Evaluation of stray current from a DC-electrified railway with integrated electric-electromechanical modeling and traffic simulation. IEEE Transactions on Industry Applications, 2015, 51(6): 5431-5441.
[11] WANG Y Q. Study on Metro stray current distributing and corrosion intelligent monitoring method. Xuzhou: China University of Mining and Technology, 2012.
[12] CHARALAMBOUS C A, AYLOTT P, BUXTON D. Stray current calculation and monitoring in dc mass-transit systems: interpreting calculations for real-life conditions and determining appropriate safety margins. IEEE Vehicular Technology Magazine, 2016, 11(2): 24-31.
[13] DU G F, WANG J, JIANG X X, et al. Evaluation of rail potential and stray current with dynamic traction networks in multitrain subway systems. IEEE Transactions on Transportation Electrification, 2020, 6(2): 784-796.
[14] LOU J J, ZHANG D L. Dynamic distribution of rail potential and stray current in urban rail transit. Journal of Beijing Jiaotong University, 2020, 44(3): 43-49.
[15] CHARALAMBOUS C A, AYLOTT P. Dynamic stray current evaluations on cut-and-cover sections of DC metro systems. IEEE Transactions on Vehicular Technology, 2014, 63(8): 3530-3538.
[16] LI Y G, LI J P, YUAN H M. Study on the Real-time Monitoring System of Laboratory Simulation of Metro Stray Current. China Railway Science, 2005, 26(5): 119-122.
[17] LI Y G, LI J P. Analog real-time monitoring system for subway stray current detection. Control Engineering of China, 2004, 11(S2): 150-152.
[18] CAO A L. Protection against stray current corrosion of buried metals pipeline. Chongqing: Chongqing University, 2010.
[19] LI M. Study on stray current of DC traction power supply system for urban rail transit. Lanzhou: Lanzhou Jiaotong University, 2020.
[20] ZHOU M, WANG J G, HUANG S B, et al. Experimental investigation on influencing factors in soil resistivity measurement. Rock and Soil Mechanics, 2011, 32(11): 3269-3275.
[21] WANG Y Q, HUANG Y J, PENG C K, et al. Evaluation model for dynamic interference of subway stray current based on surface potential gradient. Journal of Beijing Jiaotong University, 2020, 44(3): 30-36.
[22] ZHU F, LI J, ZENG H S, et al. Influence of rail-to-ground resistance of urban transit systems on distribution characteristics of stray current. High Voltage Engineering, 2018, 44(8): 2738-2745.

改进型城市轨道交通杂散电流实验平台的设计与验证

李亚宁[1*], 康　宏[1], 王　烨[2], 李文飞[1], 焦　蒙[1], 张文财[1]

1. 兰州交通大学 自动化与电气工程学院, 甘肃 兰州 730070;
2. 兰州交通大学 环境与市政工程学院, 甘肃 兰州 730070

摘　要: 城市轨道交通发展过程中, 杂散电流过大这一问题亟需解决。由于杂散电流分布随机且难以进行现场验证, 本研究对原有杂散电流实验平台进行了改进, 以真实土壤环境模拟水溶液, 通过测量土壤电阻率对过渡电阻进行计算, 以弥补现有文献的不足。首先, 建立“钢轨-排流网”及“钢轨-排流网-大地”数学模型, 并对钢轨、排流网等结构的电流、电压解析表达式进行推导。其次, 搭建仿真模型, 将数学解析结果与仿真结果进行对比验证。再次, 将实测与仿真结果进行对比, 对改进型杂散电流实验平台的准确性进行验证。最后, 基于实验结果对杂散电流的影响因素进行分析。相关结论为城市轨道交通杂散电流的研究提供了实验数据与理论参考。

关键词: 城市轨道交通; 杂散电流; 实验平台; 过渡电阻; 土壤电阻率

引用格式: LI Yaning, KANG Hong, WANG Ye, et al. Design and verification of an improved experimental platform for stray current in urban rail transit. Journal of Measurement Science and Instrumentation, 2024, 15(3): 379-386.